University of Nebraska - Lincoln
DigitalCommons@University of Nebraska - Lincoln

Peter Dowben Publications | Research Papers in Physics and Astronomy

2011

Resonant photoemission of rare earth doped GaN thin films

S. R. McHale
Air Force Institute of Technology, stephen.mchale@afit.edu

J. W. McClory
Air Force Institute of Technology, john.mcclory@afit.edu

J. C. Petrosky
Air Force Institute of Technology, James.Petrosky@afit.edu

J. Wu
University of Puerto Rico

R. Palai
University of Puerto Rico

See next page for additional authors

Follow this and additional works at: https://digitalcommons.unl.edu/physicsdowben

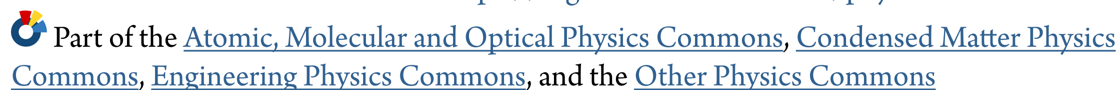
Part of the Atomic, Molecular and Optical Physics Commons, Condensed Matter Physics Commons, Engineering Physics Commons, and the Other Physics Commons

McHale, S. R.; McClory, J. W.; Petrosky, J. C.; Wu, J.; Palai, R.; Losovyj, Yaroslav B.; and Dowben, Peter A., "Resonant photoemission of rare earth doped GaN thin films" (2011). *Peter Dowben Publications*. 250.
https://digitalcommons.unl.edu/physicsdowben/250

This Article is brought to you for free and open access by the Research Papers in Physics and Astronomy at DigitalCommons@University of Nebraska - Lincoln. It has been accepted for inclusion in Peter Dowben Publications by an authorized administrator of DigitalCommons@University of Nebraska - Lincoln.

Authors
S. R. McHale, J. W. McClory, J. C. Petrosky, J. Wu, R. Palai, Yaroslav B. Losovyj, and Peter A. Dowben

This article is available at DigitalCommons@University of Nebraska - Lincoln: https://digitalcommons.unl.edu/physicsdowben/250

Eur. Phys. J. Appl. Phys. **56**, 11301 (2011)
DOI: 10.1051/epjap/2011110235

THE EUROPEAN PHYSICAL JOURNAL
APPLIED PHYSICS

Regular Article

Resonant photoemission of rare earth doped GaN thin films

S.R. McHale[1,a], J.W. McClory[1,b], J.C. Petrosky[1], J. Wu[2], R. Palai[2], Ya.B. Losovyj[3], and P.A. Dowben[4]

[1] Air Force Institute of Technology, 2950 Hobson Way, Wright Patterson Air Force Base, OH 45433, USA
[2] Department of Physics and Institute for Functional Nanomaterials, University of Puerto Rico, San Juan, PR 00931, USA
[3] The J. Bennett Johnston Sr. Center for Advanced Microstructures and Devices, Louisiana State University, 6890 Jefferson Highway, Baton Rouge, LA 70806, USA
[4] Department of Physics and Astronomy, Nebraska Center for Materials and Nanoscience, Theodore Jorgensen Hall, 855 North 16th Street, University of Nebraska, P.O. Box 880299, Lincoln, NE 68588-0299, USA

Received: 26 May 2011 / Received in final form: 7 June 2011 / Accepted: 21 June 2011
Published online: 28 September 2011 – © EDP Sciences 2011

Abstract. The $4d \rightarrow 4f$ Fano resonances for various rare earth doped GaN thin films (RE = Gd, Er, Yb) were investigated using synchrotron photoemission spectroscopy. The resonant photoemission Fano profiles show that the major Gd and Er rare earth $4f$ weight is at about 5–6 eV below the valence band maximum, similar to the $4f$ weights in the valence band of many other rare earth doped semiconductors. For Yb, there is very little resonant enhancement of the valence band of Yb doped GaN, consistent with a largely $4f^{14}$ occupancy.

1 Introduction

During the past decade, rare earth doped semiconductors have generated considerable attention for their application in new optoelectronic devices [1–4]. III-nitride semiconductors, such as AlN, GaN, and InN, offer tunable bandgaps and favorable thermal, chemical, and electronic properties, which facilitate various device applications [5–9] from the ultraviolet through the visible spectrum to the infrared range. Moreover, thin film electroluminescent phosphors with red, blue, and green emissions [7–15] imply the promise of full color (white) light capability. Rare earth doping GaN might have a number of advantages: there is the promise that Eu or Er doping will improve the light output. Luminescence due to the Er intra-$4f$-shell transition from the $^4I_{13/2}$ excited state to the $^4I_{15/2}$ ground state is known to be particularly intense and, above all, efficient. Due to their highly localized $4f$ electrons [16,17], the direct f-f interactions between the neighboring rare earth atoms are very weak and nonexistent in a weakly doped semiconductor host. In addition, rare earth doping is seen to increase the gold electrode Schottky barrier heights significantly [18] thereby decreasing leakage currents in particle type detector devices.

While numerous resonant photoemission studies of rare earth metals have been reported, the resonant processes resulting from photon interaction with III-nitride semiconductors are significantly less understood. Plucinski et al. [19] reported a resonant photoemission process at the Ga $3p$ absorption threshold in GaN and compared the results to those reported for GaP and GaAs [20,21]. Lastly, Maruyama et al. [22] reported on Eu doped GaN using X-ray photoelectron spectroscopy (XPS) and resonant photoemission spectroscopy (RPES) and concluded, via $4d \rightarrow 4f$ resonant photoemission measurements, that the transition from trivalent to divalent Eu ions occurred near the surface of GaN. The key value of resonant photoemission, however, is to probe what valence bands of the semiconductors have strong $4f$ and/or rare earth weight [23–25]. Of course, such photon energy dependent studies must be disentangled from bulk band structure effects, so there is considerable value in studying the resonant photoemission process of a semiconductor with several different rare earths; each is likely to dope the semiconductor in a similar fashion, but the resonant enhancement of the valence band will occur at different photon energies.

Although likely to locally strain the lattice, the $4f$ rare earths will tend to adopt substitutional sites for Ga [1,2,26] in GaN while significantly altering magnetic [27–34] and optical properties [7–14], and it is therefore of considerable interest to know whether even low concentrations of a rare earth in the GaN host can alter the surface electronic structure. This is likely, as although rare earths are isoelectronic with Ga^{3+}, they may be associated with other defects [35,36]. With these considerations in mind, we have engaged in investigations of the surface electronic structure and interface properties of the $RE_xGa_{1-x}N$ (RE = Gd, Er, Yb) semiconductors.

[a] e-mail: stephen.mchale@afit.edu
[b] e-mail: john.mcclory@afit.edu

2 Experimental

The $RE_xGa_{1-x}N$ thin films (50–300 nm) were fabricated on Si(1 1 1) (RE = Gd, Yb) and sapphire Al_2O_3 (RE = Er) substrates by RF plasma (EPI 620) assisted molecular beam epitaxy (MBE). The growth parameters for the deposition of RE-doped (in situ) GaN thin films were base pressure of $\sim 10^{-11}$ Torr, nitrogen flux of 0.75–1.0 SCCM (Gd, Yb) and 2.0 SCCM (Er), RF power of 500 W, substrate temperature of 850–900 °C, Ga cell temperature of 850 °C, and RE cell temperatures of 1050–1100 °C (Gd), 1000–1100 °C (Er), and 500–850 °C (Yb). The thickness of the films was measured with a surface profilometer and by atomic force microscopy.

The orientation, crystal structure, and phase purity of the films were established by Cu K_α (λ = 1.5406 Å) radiation X-ray diffraction using a Siemens D5000 X-ray diffractometer. The X-ray diffraction (XRD) patterns of Gd, Er, and Yb doped GaN films show c-axis orientation and a high degree of crystallinity. The presence of any secondary phases or spurious peaks has not been observed, as described elsewhere [18]. Slight shifts in diffraction peak positions toward lower Bragg angles have been observed with Er doped GaN grown on Al_2O_3(0 0 0 1) substrates and $RE_xGa_{1-x}N$ thin films (50–300 nm) fabricated on Si(1 1 1) (RE = Gd, Yb), which is indicative of some lattice expansion, as is expected [26]. The c-axis length of GaN:Yb was found to be 5.172 Å [26], which is very close to the widely reported and accepted c-axis length (5.166 Å) of undoped GaN.

The elemental compositions of the rare earth doped GaN thin films grown under different conditions were characterized by energy dispersive spectroscopy (EDS) and a VG Microtech XPS attached to the MBE growth system (VG Microtech). The measured concentrations were found to be at 1–2%, as confirmed from the Ga $2p_{3/2}$, Er $4d$, Gd $4d$, Yb $4d$, and N $1s$ core level XPS intensities using an Al K_α (1486.8 eV) X-ray source. The typical values for Er concentrations were found to be ∼5%, higher than the EDS- and XPS-derived Gd and Yb concentrations. In the rare earth doped GaN samples, surface segregation cannot be excluded and may well be likely, at least in the selvedge region of the surface.

The photoemission experiments were conducted on the 3 m TGM beamline [37] at the Center for Advanced Microstructures and Devices at Louisiana State University [38–40]. The beamline is equipped with a photoemission endstation with a 50 mm hemispherical electron energy analyzer, with a resolution of about 70 meV, as described elsewhere [37,41]. Photoemission spectra were taken with a 45° incidence angle and the photoelectrons collected along the sample normal. All spectra presented are normalized to the photon flux, and the secondary electron background has been subtracted. The position of the Fermi level was established using a clean Ta foil as reference. All binding energies reported here are with respect to this common Fermi level in terms of $E - E_F$, so that occupied state binding energies are negative. Energy distribution curves (EDCs) were obtained by fixing the photon energy $h\nu$ and sweeping electron kinetic energy E_K, thus measuring binding energies. Constant initial state spectra were obtained by simultaneously sweeping $h\nu$ and E_K, so as to hold binding energy fixed.

Atomically clean GaN:RE surfaces were obtained by several preparatory cycles of Ar^+ ion sputtering and annealing, as described elsewhere [18,26]. This will create a number of point defects, but photoemission is generally insensitive to such defects. The photoemission spectra from the clean sample surfaces indicated that the surfaces were free of contaminants.

3 Results and discussion

3.1 Identification of the 4*f* contributions to the valence band of doped GaN

The effects of band hybridization and dopant-induced strain between the various rare earth dopants and the GaN surfaces are not identical. The valence band spectra for Gd and Er doped GaN are very similar as seen in Figures 1 and 2, while for Yb doped GaN (Fig. 3), the valence band is significantly broader extending from −2 eV to nearly −14 eV. The spectra do change with photon energy and significant enhancements of some of the valence band features are seen at some photon energies. Figures 1–3 (RE = Gd, Er, Yb) show the valence band photoemission spectra at various photon energies in the vicinity of the respective rare earth dopant $4d$ absorption thresholds. For the rare earth dopants studied, resonance results from a signal overlap between direct emission of photoelectrons from the $4f$ state

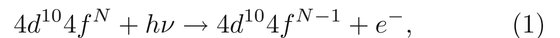

$$4d^{10}4f^N + h\nu \rightarrow 4d^{10}4f^{N-1} + e^-, \quad (1)$$

and Auger-like electrons emitted in a super Coster-Kronig process [42]

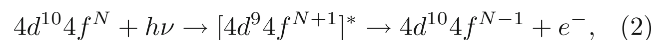

$$4d^{10}4f^N + h\nu \rightarrow [4d^9 4f^{N+1}]^* \rightarrow 4d^{10}4f^{N-1} + e^-, \quad (2)$$

where [ ]* denotes an excited state. The final states for both the direct and recombination processes are identical.

For Gd doped GaN (GaN:Gd), Figure 1 shows that the intensity of the spectral features near 8–9 eV below the Fermi level first increases slightly at ∼144 eV, followed by a rapid and coenhancement, with maximum intensity at a photon energy of ∼148 eV. Figure 2 shows a similar, albeit not identical, response for GaN:Er. As with the GaN:Gd thin film, the spectral feature at an approximate binding energy of −9 eV in GaN:Er resonates in the range of the Er $4d$ absorption threshold. However, Figure 2 shows that the features near the bottom of the valence band increase in intensity considerably first at ∼165 eV and then again at ∼176 eV for GaN:Er. Lastly, Figure 3 (GaN:Yb) reveals that the intensity of spectral features at binding energy ∼7 eV increases slightly at ∼178 eV, and slightly again at ∼190 eV.

The intensity of the valence band features for which the direct and super Coster-Kronig processes overlap is

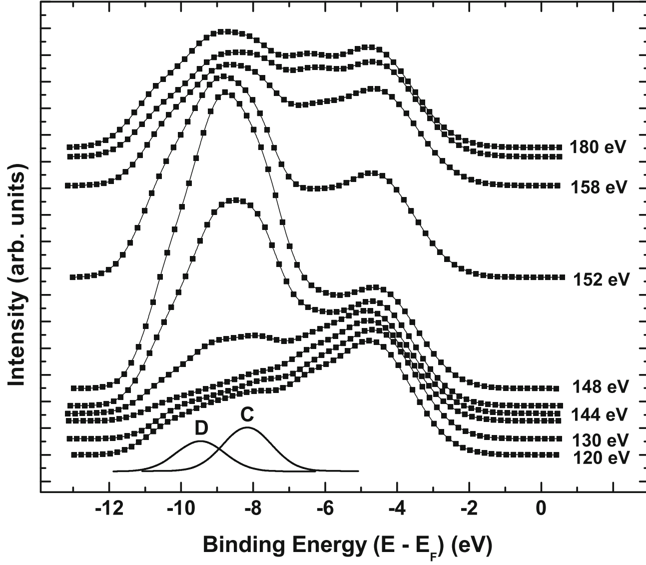

Fig. 1. Energy distribution curves of GaN:Gd for various incident photon energies, as shown for each spectrum. The strong surface and bulk $4f$ Gd components of the GaN:Gd valence band are illustrated. Resonating components C (-8.1 eV) and D (-9.6 eV), used for the constant initial state curves in Figure 4, are shown at the bottom.

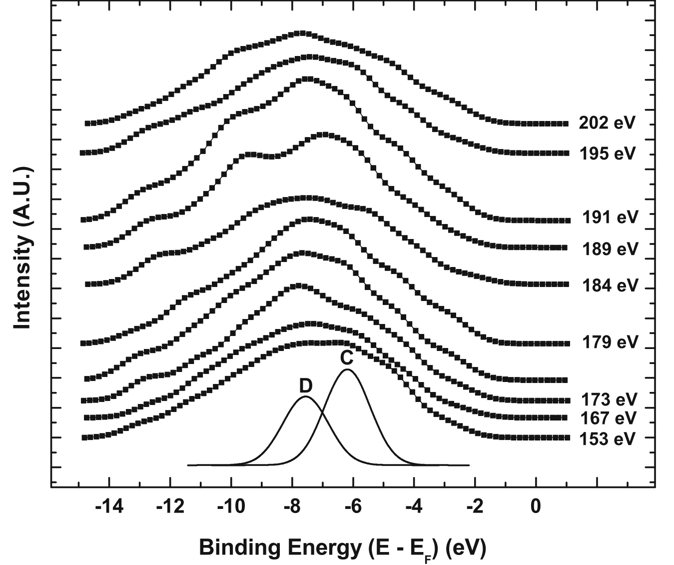

Fig. 3. Energy distribution curves of GaN:Yb for various incident photon energies, as shown for each spectrum. Resonating components C (-6.2 eV) and D (-7.6 eV), used for the constant initial state curve in Figure 5, are shown at the bottom.

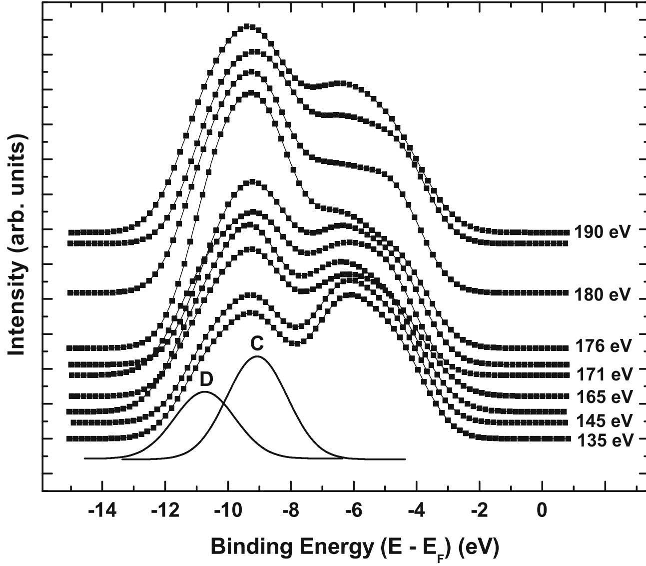

Fig. 2. Energy distribution curves of GaN:Er for various incident photon energies, as shown for each spectrum. The resonating components C (-8.9 eV) and D (-10.7 eV), used for the constant initial state curve in Figure 6, are shown at the bottom.

described as a function of photon energy $h\nu$ by the Fano lineshape [42,43] as

$$N(h\nu) \cong \frac{(\epsilon+q)^2}{\epsilon^2+1}, \quad \epsilon = \frac{h\nu - h\nu_j}{\Gamma}, \tag{3}$$

where $h\nu_j$ is the photon energy equal to the core level absorption threshold binding energy, q is a fitting parameter for the core level, and $\Gamma = \Delta(h\nu_j)/2$ where $\Delta(h\nu_j)$ is the width (FWHM) of the core level.

3.2 Identification of the 4*f* contributions to the valence band of GaN:Gd

The GaN:Gd valence band components, at binding energies in the region of -8 to -10 eV, represent the valence band features that strongly resonate at photon energies in the vicinity of 147 eV, as plotted in Figure 4. These intensity resonances (Fig. 4) are very similar to those observed for Gd_2O_3 [44] and Gd doped HfO_2 [23,44]. Not only are the resonant photon energies similar, but the features at the bottom of the valence band contain a strong feature at about -8 eV binding energy and a weaker shoulder in the vicinity of -10 eV binding energy. This suggests a surface and bulk component for the Gd in GaN, in spite of the low Gd concentrations. Figure 4 displays the constant initial state spectra and the calculated Fano profiles for GaN:Gd. The weighted oscillator strength, *gf*, relates directly to the electric dipole transition probability and, hence, line intensity. Theoretical interpretations of resonant photoemission in lanthanide metals at the $4d$ absorption threshold via *gf* calculations have been reported [45] and have been shown to agree well with experimental results [46]. The resonance peak, at roughly 147.5 eV for the GaN:Gd Fano line profile in Figure 4, illustrates reasonable agreement with the Gd *gf* calculations of Sugar [45], which indicated a strong absorption peak centered at 149.0 eV. This agreement supports further the assertion that the GaN:Gd spectral features at the bottom of the valence band, in the region of -8 to -10 eV in Figure 1, are of strong Gd $4f$ weight or represent bands that strongly hybridize with the rare

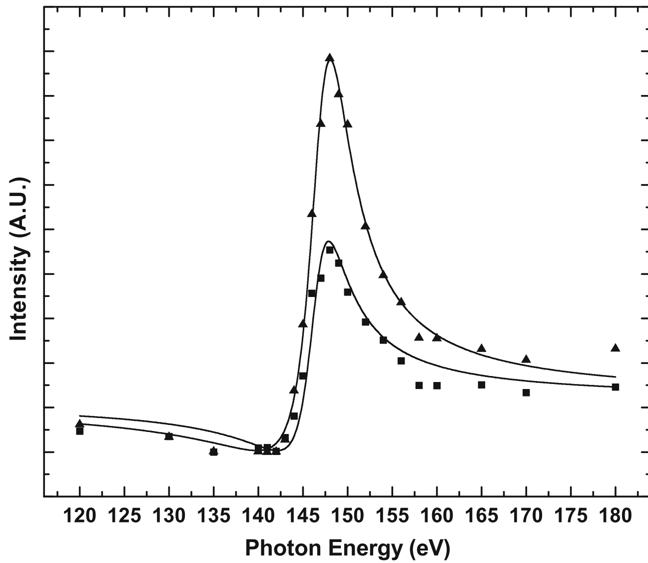

Fig. 4. Constant initial state curves and Fano fit (solid lines) for feature C (■) at −8.1 eV and feature D (▲) at −9.6 eV in GaN:Gd. The fitting component, q, for feature C was calculated as 1.91; for feature D it was 2.79.

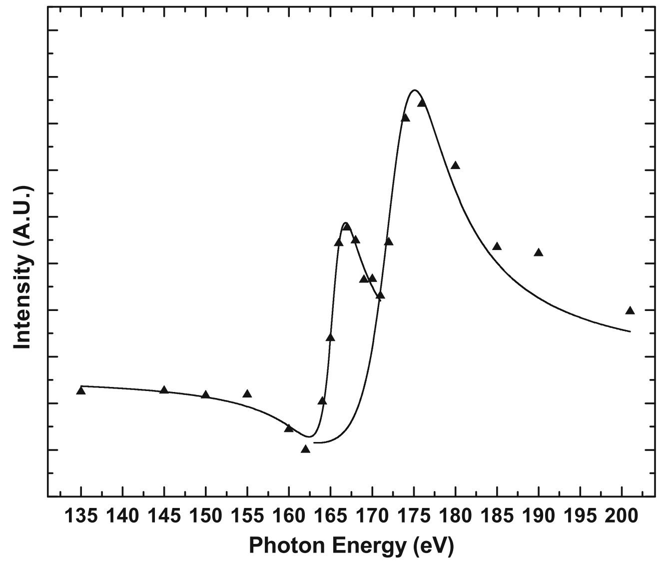

Fig. 5. Constant initial state curve (▲) and Fano fit (solid lines) for the valence band feature in the vicinity of −9 eV binding energy, for GaN:Er. The fitting component, q, in the region of the Er $4d_{5/2}$ absorption threshold (166 eV) was calculated as 1.55; in the region of the Er $4d_{3/2}$ absorption threshold (173 eV) it was 2.14.

earth. This is expected based on the Gd occupied $4f$ level placement in GdN [27,47].

3.3 Identification of the 4*f* contributions to the valence band of GaN:Er

Similarly, for GaN:Er, the valence band features, again at the bottom of the valence band at binding energies of roughly −8.9 and −10.7 eV, strongly resonate at photon energies of 166 and 173 eV, as plotted in Figure 5. Two Fano lineshapes were used to fit the experimental results for GaN:Er, shown in Figure 5. The GaN:Er Fano line profile in Figure 5 also shows reasonable agreement with the gf calculations [45]. Specifically, Sugar reported the separation between oscillator strength maxima at 167.2 eV and 174.8 eV to be 7.6 eV for Er [45]. Our experimentally observed separation is roughly 7–7.5 eV between absorption peaks at 166 eV and 173 eV for GaN:Er. The ratio of the Er computational peak maxima reported by Sugar is ∼1:2.6 [45], somewhat larger than the ratio of the peak maxima at roughly 166 eV and 173 eV of about $1.55^2/2.14^2$ or ∼1:1.9 for GaN:Er, as plotted in Figure 5. Although inspection of equation (3) predicts that when $h\nu \to h\nu_j$, $N(h\nu) \to q^2$, nonetheless, the resonant photoemission of the GaN:Er thin film at absorption thresholds of roughly 166 eV and 173 eV represents reasonable agreement with the Er $4d$ shallow core (167.2 eV, 174.8 eV) binding energies. Thus, unlike the case of the Gd doped GaN, there are spin-orbit interactions that separate out the $4d_{3/2}$ and $4d_{5/2}$ in GaN:Er.

Judging by ErAs [48], we would expect $4f$ contributions at both the bottom and the top of the valence band of GaN. The region of 4–6 eV binding energy should be dominated by the $4f_{7/2}$ (mainly the $^5I_8$ and $^5I_7$ multiplet components [48–50]), while the bottom of the valence band should be dominated by the $4f_{5/2}$ (mainly the $^3M_{10}$ and $^3L_9$ multiplet components [48–50], although there are many others). In fact, the f removal energies calculated for Er placed in GaN are seen to be very similar to those noted for Gd in GaN [51]. While there are indications that the occupied density of states would have the spectral weight density at the bottom of the valence band, although complexed with a vacancy defect, contributions at the top of the valence band might also be expected [36]. This differs from the relative position of the Gd and Er $4f$ levels in GaAs [51]. Strong hybridization of the $4f$ states, possibly modified by intra-atomic f-d and f-s hybridizations [48,52–54], can lead to a much more delocalized core exciton, and a decrease in the resonant photoemission intensities [55].

3.4 Identification of the 4*f* contributions to the valence band of GaN:Yb

To test the possibility of intra-atomic f-d and f-s hybridizations [48,52–54], or extra-atomic $4f$ hybridization with the Ga and N, we also looked at the resonant enhancement of the valence band of GaN:Yb, as seen in Figures 3 and 6. Although much weaker than the resonant enhancements observed for GaN:Gd (Fig. 4) and GaN:Er (Fig. 5), there is a resonant enhancement of the valence band, particularly in the region of approximately −6 to −7 eV binding energy, as plotted in Figure 6. Although Yb metal should have an electronic configuration of $4d^{10}4f^{14}$, such that an excited $4d$ electron has no unfilled $4f$ state to occupy, partial $4f$ occupancy is still possible. Previous experimental results [56,57] using the oxidation-induced

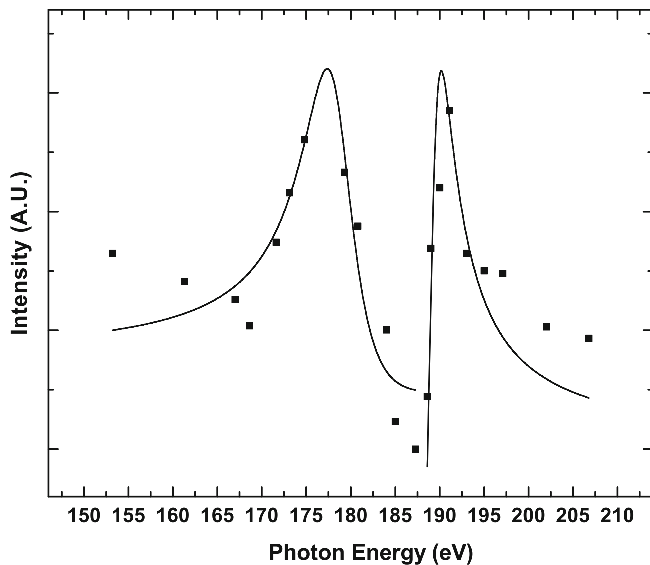

Fig. 6. Constant initial state curve (■) and Fano fit (solid lines) for the valence band features in the vicinity of −7 eV binding energy, for GaN:Yb. The fitting component, q, in the region of the Yb $4d_{5/2}$ absorption threshold (179 eV) was calculated as 0.33; in the region of the Yb $4d_{3/2}$ absorption threshold (189 eV) it was 1.15.

valence change of Yb ($4f^{14} \rightarrow 4f^{13}$) determined that the data for Yb_2O_3 were well described by Fano's theory of interaction between discrete and continuum states. There are similar expectations for Er doped GaSb [58]. Despite the relative weakness of the observed Fano lineshapes for GaN:Yb, we note that the enhancements in spectral features in the valence band do exhibit photoemission resonances at photon energies in the vicinity of 179 eV and 189 eV. These absorption thresholds agree reasonably well with the Yb $4d_{5/2}$ (182.0 eV) and the Yb $4d_{3/2}$ (190.8 eV) shallow core level binding energies. Because it is not just the valence band maximum that exhibits the weak photoemission resonance in the expected location of the Yb $4f$ multiplets [49], the depletion of the $4f$ occupancy appears related to strong hybridization with the GaN lattice.

4 Summary and conclusions

Resonant photoemission for GaN thin films doped with various rare earths (RE = Gd, Er, Yb) was investigated using synchrotron-based photon energy dependent photoemission spectroscopy. The calculated Fano profiles predict the experimentally observed $4d \rightarrow 4f$ super Coster-Kronig processes and strong rare earth $4f$ weights were observed about 5–6 eV below the valence band maximum for Gd and Er doped GaN. For Yb, the photoemission resonance is much weaker, indicating that there is only a very little depletion of the $4f^{14}$ occupancy, but strong hybridization with GaN is implicated. There is also evidence from the selectivity of the resonant photoemission enhancement of the valence band that there is also strong $4f$ hybridization with the GaN valence bands, particularly within the Er $4f_{5/2}$ envelope. The results here on the placement of the occupied Gd, Er and Yb $4f$ levels, deep within the valence band, suggest that the intra-atomic f-f transitions may be more 'blue' than predicted by many theoretical models. The resonant photoemission results strongly support the predicted hybridization with the host lattice [54], and the expected f-s hybridization [48,52–54].

This work was supported by the Defense Threat Reduction Agency (DTRA) through Grant Nos. HDTRA1-07-1-0008 and BRBAA08-I-2-0128, the Nebraska Materials Science and Engineering Center (DMR-0820521), the Institute for Functional Nanomaterials, and NASA-IDEA-PR. Additional support for undergraduates, at UNL, was provided by DMR-0851703. The J. Bennett Johnston Sr. Center for Advanced Microstructures and Devices (CAMD) is supported by the Louisiana Board of Regents.

The views expressed in this article are those of the authors and do not reflect the official policy or position of the Air Force, Department of Defense, or the U.S. Government.

References

1. T. Koubaa, M. Dammak, M. Kammoun, W.M. Jadwisienczak, H.J. Lozykowski, J. Alloys Compd. **496**, 56 (2010)
2. T. Koubaa, M. Dammak, M. Kammoun, W.M. Jadwisienczak, H.J. Lozykowski, A. Anders, J. Appl. Phys. **106**, 013106 (2009)
3. W.M. Jadwisienczak, H.J. Lozykowski, Opt. Mater. **23**, 175 (2003)
4. A.J. Kenyon, Prog. Quant. Electr. **26**, 225 (2002)
5. J.H. Park, A.J. Steckl, Phys. Stat. Sol. (a) **205**, 26 (2008)
6. A. Nishikawa, T. Kawasaki, N. Furukawa, Y. Terai, Y. Fujiwara, Appl. Phys. Exp. **2**, 1004 (2009)
7. A.J. Steckl, J. Heikenfeld, D.S. Lee, M. Garter, Mater. Sci. Eng. B **81**, 97 (2001)
8. J.H. Tao, N. Perea-Lopez, J. McKittrick, J.B. Talbot, K. Klinedinst, M. Raukas, J. Laski, K.C. Mishra, G. Hirata, Phys. Stat. Sol. (c) **5**, 1889 (2008)
9. J. Shi, M.V.S. Chandrashekhar, J. Reiherzer, W. Schaff, J. Lu, F. Disalvo, M. Spencer, Phys. Stat. Sol. (c) **5**, 1495 (2008)
10. W. Jadwisienczak, K. Wisniewski, M. Spencer, T. Thomas, D. Ingram, Radiat. Meas. **45**, 500 (2010)
11. H. Okada, Y. Nakanishi, A. Wakahara, A. Yoshida, T. Ohshima, Nucl. Instr. Methods B **266**, 853 (2008)
12. Y. Nakanishi, A. Wakahara, H. Okada, A. Yoshida, T. Ohshima, H. Itoh, Appl. Phys. Lett. **81**, 1943 (2002)
13. T. Thomas, X. Guo, M.V.S. Chandrashekhar, C.B. Poitras, W. Shaff, M. Dreibelbis, J. Reiherzer, K. Li, F.J. DiSalvo, M. Lipson, J. Cryst. Growth **311**, 4402 (2009)
14. A.J. Steckl, J.H. Park, J.M. Zavada, Mater. Today **10**, 20 (2007)
15. Y.Q. Wang, A.J. Steckl, Appl. Phys. Lett. **82**, 502 (2003)
16. G.H. Dieke, H.M. Crosswhite, Appl. Opt. **2**, 675 (1963)
17. S. Hüfner, K.A. Gschneidner, L.R. Eyring, *Handbook on the Physics and Chemistry of Rare Earths* (North Holland, Amsterdam, 1978)

18. S.R. McHale, J.W. McClory, J.C. Petrosky, J. Wu, A. Rivera, R. Palai, Y.B. Losovyj, P.A. Dowben, Eur. Phys. J. Appl. Phys. **53**, 31301 (2011)
19. L. Plucinski, T. Learmonth, L. Colakerol, S. Bernardis, Y. Zhang, P.A. Glans, K.E. Smith, A.A. Zakharov, R. Nyholm, I. Grzegory, Solid State Commun. **136**, 191 (2005)
20. T.C. Chiang, D.E. Eastman, Phys. Rev. B **21**, 5749 (1980)
21. S. Suzuki, T. Kiyokura, F. Maeda, K.G. Nath, Y. Watanabe, T. Saitoh, A. Kakizaki, J. Electron Spectros. Relat. Phenomena **114**, 421 (2001)
22. T. Maruyama, S. Morishima, H. Bang, K. Akimoto, Y. Nanishi, J. Cryst. Growth **237**, 1167 (2002)
23. I. Ketsman, Y.B. Losovyj, A. Sokolov, J. Tang, Z. Wang, K.D. Belashchenko, P.A. Dowben, Appl. Phys. A: Mater. Sci. Process. **89**, 489 (2007)
24. R.F. Sabirianov, W.N. Mei, J. Lu, Y. Gao, X.C. Zeng, R.D. Bolskar, P. Jeppson, N. Wu, A.N. Caruso, P.A. Dowben, J. Phys.: Condens. Matter **19**, 082201 (2007)
25. I. Ketsman, Y.B. Losovyj, A. Sokolov, J. Tang, Z. Wang, M.L. Natta, J.I. Brand, P.A. Dowben, Appl. Surf. Sci. **254**, 4308 (2008)
26. S.R. McHale, J.W. McClory, J.C. Petrosky, J. Wu, R. Palai, P.A. Dowben, I. Ketsman, Mater. Lett. **65**, 1476 (2011)
27. C.G. Duan, R.F. Sabirianov, W.N. Mei, P.A. Dowben, S.S. Jaswal, E.Y. Tsymbal, J. Phys.: Condens. Matter **19**, 315220 (2007)
28. H. Asahi, Y.K. Zhou, M. Hashimoto, M.S. Kim, X.J. Li, S. Emura, S. Hasegawa, J. Phys.: Condens. Matter **16**, S5555 (2004)
29. M. Takahashi, Y.K. Zhou, T. Nakamura, S. Emura, S. Hasegawa, H. Asahi, J. Supercond. Nov. Magn. **23**, 107 (2010)
30. S. Dhar, O. Brandt, M. Ramsteiner, V.F. Sapega, K.H. Ploog, Phys. Rev. Lett. **94**, 37205 (2005)
31. L. Pérez, G.S. Lau, S. Dhar, O. Brandt, K.H. Ploog, Phys. Rev. B **74**, 195207 (2006)
32. J. Hejtmánek, K. Knížek, M. Maryško, Z. Jirák, D. Sedmidubský, Z. Sofer, V. Peřina, H. Hardtdegen, C. Buchal, J. Appl. Phys. **103**, 07D107 (2008)
33. S.Y. Han, J. Hite, G.T. Thaler, R.M. Frazier, C.R. Abernathy, S.J. Pearton, H.K. Choi, W.O. Lee, Y.D. Park, J.M. Zavada, Appl. Phys. Lett. **88**, 042102 (2006)
34. N. Teraguchi, A. Suzuki, Y. Nanishi, Y.K. Zhou, M. Hashimoto, H. Asahi, Solid State Commun. **122**, 651 (2002)
35. J.S. Filhol, R. Jones, M.J. Shaw, P.R. Briddon, Appl. Phys. Lett. **84**, 2841 (2004)
36. B. Hourahine, S. Sanna, B. Aradi, C. Köhler, T. Frauenheim, Phys. B: Condens. Matter **376**, 512 (2006)
37. Y. Losovyj, I. Ketsman, E. Morikawa, Z. Wang, J. Tang, P. Dowben, Nucl. Instrum. Methods A **582**, 264 (2007)
38. J. Hormes, J.D. Scott, V.P. Suller, Synchrotron Radiat. News **19**, 27 (2006)
39. A. Roy, E. Morikawa, H. Bellamy, C. Kumar, J. Goettert, V. Suller, K. Morris, D. Ederer, J. Scott, Nucl. Instrum. Methods A **582**, 22 (2007)
40. E. Morikawa, J.D. Scott, J. Goettert, G. Aigeldinger, C.S.S.R. Kumar, B.C. Craft, P.T. Sprunger, R.C. Tittsworth, F.J. Hormes, Rev. Sci. Instrum. **73**, 1680 (2002)
41. P.A. Dowben, D. LaGraffe, M. Onellion, J. Phys.: Condens. Matter **1**, 6571 (1989)
42. G. Wendin, *Breakdown of the One-Electron Pictures in Photoelectron Spectra, Structure and Bonding*, vol. 45 (Springer-Verlag, Berlin, 1981)
43. U. Fano, Phys. Rev. **124**, 1866 (1961)
44. Y.B. Losovyj, D. Wooten, J.C. Santana, J.M. An, K.D. Belashchenko, N. Lozova, J. Petrosky, A. Sokolov, J. Tang, W. Wang, J. Phys.: Condens. Matter **21**, 045602 (2009)
45. J. Sugar, Phys. Rev. B **5**, 1785 (1972)
46. T.M. Zimkina, V.A. Fomichev, S.A. Gribovskii, I.I. Zhukova, Sov. Phys. Solid State **9**, 1447 (1967)
47. F. Leuenberger, A. Parge, W. Felsch, K. Fauth, M. Hessler, Phys. Rev. B **72**, 014427 (2005)
48. T. Komesu, H.K. Jeong, J. Choi, C.N. Borca, P.A. Dowben, A.G. Petukhov, B.D. Schultz, C.J. Palmstrm, Phys. Rev. B **67**, 035104 (2003)
49. J.K. Lang, Y. Baer, P.A. Cox, J. Phys. F: Metal Phys. **11**, 121 (1981)
50. L. Stauffer, C. Pirri, P. Wetzel, A. Mharchi, P. Paki, D. Bolmont, G. Gewinner, C. Minot, Phys. Rev. B **46**, 13201 (1992)
51. A. Svane, N.E. Christensen, L. Petit, Z. Szotek, W.M. Temmerman, Phys. Rev. B **74**, 165204 (2006)
52. I.N. Yakovkin, T. Komesu, P.A. Dowben, Phys. Rev. B **66**, 035406 (2002)
53. P. Strange, A. Svane, W.M. Temmerman, Z. Szotek, H. Winter, Nature **399**, 756 (1999)
54. G.M. Dalpian, S.H. Wei, Phys. Rev. B **72**, 115201 (2005)
55. P.A. Dowben, Surf. Sci. Rep. **40**, 151 (2000)
56. L.I. Johansson, J.W. Allen, I. Lindau, M.H. Hecht, S.B.M. Hagström, Phys. Rev. B **21**, 1408 (1980)
57. J. Schmidt-May, F. Gerken, R. Nyholm, L.C. Davis, Phys. Rev. B **30**, 5560 (1984)
58. Y.M. Sun, M.C. Wu, J. Appl. Phys. **78**, 6691 (1995)